PHILOSOPHICAL TRANSACTIONS OF THE ROYAL SOCIETY B BIOLOGICAL SCIENCES

Aggregation and collapse of fungal wall vesicles in hyphal tips: a model for the origin of the Spitzenkorper

Carlos M. Regalado, Brian D. Sleeman and Karl Ritz

Phil. Trans. R. Soc. Lond. B 1997 **352**, 1963-1974
doi: 10.1098/rstb.1997.0182

Aggregation and collapse of fungal wall vesicles in hyphal tips: a model for the origin of the Spitzenkörper

CARLOS M. REGALADO[1*], BRIAN D. SLEEMAN[2] AND KARL RITZ[1]

[1] *Centre for Nonlinear Systems in Biology, Unit of Integrative Bioscience, Cellular and Environmental Physiology Department, Scottish Crop Research Institute, Invergowrie, Dundee DD2 5DA, UK* (cregal@scri.sari.ac.uk)

[2] *Department of Applied Mathematical Studies, University of Leeds, Leeds LS2 9JT, UK*

CONTENTS

SUMMARY

The intracellular origins of polarity and branch initiation in fungi centre upon a localization in the supply of fungal wall constituents to specific regions on the hyphal wall. Polarity is achieved and maintained by accumulating secretory vesicles, prior to incorporation into the wall, in the form of an apical body or Spitzenkörper. However, neither the mechanisms leading to this accumulation nor the initiation of branching, are as yet understood. We propose a mechanism, based on experimental evidence, which considers the mechanical properties of the cytoskeleton in order to explain these phenomena. Cytoskeletal viscoelastic forces are hypothesized to be responsible for biasing vesicles in their motion, and a mathematical model is derived to take these considerations into account. We find that, as a natural consequence of the assumed interactions between vesicles and cytoskeleton, wall vesicles aggregate in a localized region close to the tip apex. These results are used to interpret the origin of the Spitzenkörper. The model also shows that an aggregation peak can collapse and give rise to two new centres of aggregation coexisting near the tip. We interpret this as a mechanism for apical branching, in agreement with published observations. We also investigate the consequences and presumptive role of vesicle–cytoskeleton interactions in the migration of satellite Spitzenkörper. The results of this work strongly suggest that the formation of the Spitzenkörper and the series of dynamical events leading to hyphal branching arise as a consequence of the bias in vesicle motion resulting from interactions with the cytoskeleton.

1. INTRODUCTION

The highly polarized and indeterminate vegetative growth characteristic of many members of the fungal kingdom have contributed significantly to its evolutionary success. It provides an essentially non-motile organism with 'mobility', morphological plasticity and the capability to spatially explore the surrounding environment (Andrews 1995; Carlile 1995). Growth of an eucarpic fungal colony is achieved by the elongation and branching of individual hyphae predominantly at the periphery of the colony (Trinci 1971). Central to the question of generation and maintenance of polarity and the initiation of branching is to understand how the shaping of a single hyphal tube occurs. Although turgor pressure might be responsible for expanding the hyphal wall (Money 1990; Kaminskyj *et al.* 1992; Money & Harold 1992), it is agreed that, in order to maintain a localized growth of the hyphal tip, the constitutive wall components must be supplied in an appropriate man-

* Author for correspondence.

ner. Thus a fundamental process governing fungal morphogenesis is the supply and inclusion of membrane, wall precursors and enzymes at the apex of hyphae. These are thought to originate in the lumen of the hyphae as vesicles derived from the endoplasmic reticulum, which travel towards the apex and ultimately fuse with the hyphal wall (figure 1*a*) (Grove & Bracker 1970; Howard 1981; Koch 1982). Thus the growth of a hyphal tube is restricted to the cytosolic activity of the most apical end of the cell, to a volume of less than 700 μm^3. In contrast, vesicles have a typical size of 40–70 nm in diameter (microvesicles) up to 90–150 nm in diameter (macrovesicles) (see Vargas *et al.* 1993 and the references therein). Given such differences in scales, it is estimated, for example, that a hyphal tube of *Neurospora crassa* extending at a characteristic rate of 38 $\mu m\ min^{-1}$ and with an extension zone of 29 μm, would require of the order of 4×10^4 vesicles to fuse per minute with the extending tip wall, in order to achieve such an elongation rate (Collinge & Trinci 1974). From these estimates, it is also evident that the speed of vesicle movement must be much greater than the rate of hyphal extension, for the vesicles to fuse with the extending hyphal wall. For example, vesicle motility takes place at about 1–10 $\mu m\ s^{-1}$ (McKerracher & Heath 1987), and Howard (1983) reported particle movement at a rate of 3 $\mu m\ s^{-1}$ in hyphal tubes of *Gilbertella*. Cytoplasmic migration (and therefore tip growth) ranges from 1–10 $\mu m\ min^{-1}$ (McKerracher & Heath 1987); more recently, finer measures of growth rate in different species of fungi give values lying between 0.038 and 0.248 $\mu m\ s^{-1}$ (López-Franco *et al.* 1994).

Wall vesicles appear concentrated just behind the apex in the form of an organized apical body or Spitzenkörper (Brunswik 1924; López-Franco & Bracker 1996), in the case of septate fungi, or in a less organized form in Oömycetes and Zygomycetes (Girbardt 1957, 1969; Grove & Bracker 1970; Grove 1978; Howard 1981; López-Franco & Bracker 1996). Vesicles may arrive at the Spitzenkörper individually or in clusters, or 'satellites' (López-Franco *et al.* 1995). Although central to the understanding of tip morphogenesis, the origin of both the Spitzenkörper and satellites is as yet unknown. An accumulation of vesicles associated with growth is also present in other tip-growing systems such as pollen tubes (Steer & Steer 1989) and root hairs (Bonnett & Newcomb 1966). It is considered that accumulation of vesicles prior to their incorporation into the wall localizes their supply (and therefore growth) to the most apical region of the tip. This phenomenon will maintain polarity, and will prevent budding, as is typical of yeast-like growth. Differences in the way material is supplied to the hyphal wall may also contribute to mechanisms which distinguish between apical branching, mycelial and pseudomycelial growth. Models such as the 'hyphoid' model (Bartnicki-Garcia *et al.* 1989), which simulate the above phenomena, are based upon the existence of an 'organizing or vesicle supply centre (VSC)'. However, they do not explain how such a VSC is initiated, nor consider what the mechanisms involved

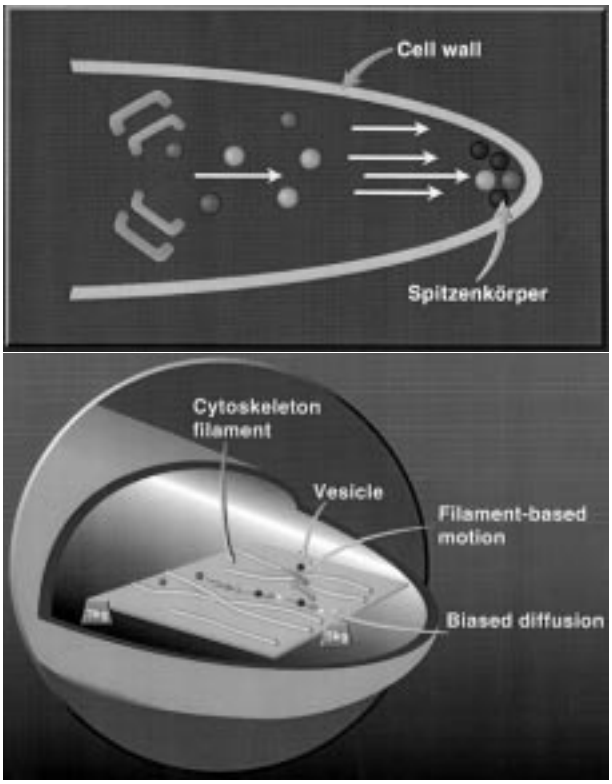

Figure 1. (Top) The growth of a hyphal tube takes place by deposition of secretory vesicles at the hyphal wall. They originate in Golgi equivalents, travel towards the apex of the tip and appear accumulated as an apical body or Spitzenkörper before fusing with the extending cell wall. (Bottom) The main hypotheses considered in the model are depicted here. Forces generated at the cytoskeleton orientate cytoskeleton filaments, and therefore facilitate the motion of vesicles along the axis of deformation (as opposed to perpendicularly to this axis): biased diffusion. The deformation of the cytoskeleton by vesicles generates a propelling force which permits their displacement: filament-based motion

in the organization and dynamics of vesicles and the VSC are. In the hyphoid model the Spitzenkörper zone is identified *a posteriori* with the VSC. Indeed the Spitzenkörper has long been thought to be responsible for the vectorial growth of the hyphal tip. Recent experimental observations of growing hyphal tips (Bartnicki-Garcia *et al.* 1989; López-Franco *et al.* 1995) strongly support this evidence.

Vesicles have no inherent motility. In order to explain their motion, extrinsic mechanisms of transport must be invoked. Little is known about the way wall vesicles are transported and although several experiments relate the cytoskeleton to the organization of the Spitzenkörper (Howard & Aist 1980; Borett & Howard 1991) and the spatial distribution of vesicles (Howard & Aist 1980; Novick & Bolstein 1985; Hoch *et al.* 1987; Heath & Kaminskyj 1989), the direct association of vesicles to single cytoskeletal filaments is far from proven (Howard 1981, 1983; Heath *et al.* 1985; Heath & Kaminskyj 1989). In this paper we propose a possible mechanism by which viscoelastic forces generated by the cytoskeleton are responsible for orienting vesicles towards the apex. Such a mech-

PHILOSOPHICAL TRANSACTIONS OF THE ROYAL SOCIETY B BIOLOGICAL SCIENCES

anism does not preclude a direct association between the cytoskeleton filaments and the wall vesicles. However, it does not depend upon such an association, in order to explain the involvement of cytoskeleton components in the spatial organization of wall vesicles. A certain degree of cytoskeletal integrity is required, and therefore vesicle transport will be affected indirectly by any disruption of the cytoskeletal network.

We begin by describing the mechanical properties of the cytoskeleton in terms of viscoelastic forces (Murray *et al.* 1983; Oster *et al.* 1983; Murray & Oster 1984*a*, *b*). We then review some experimental observations regarding the possible involvement of the cytoskeleton in the spatial organization of wall vesicles. These are then translated into a mathematical form by means of conservation equations. By coupling cytoskeletal viscoelastic forces to the vesicle conservation equation, we characterize the motion of wall vesicles and discuss the results in terms of the origin of the Spitzenkörper and apical branch initiation. The hypothesized role of cytoskeletal motors and their possible involvement in the transport *en masse* of wall vesicle clusters, is also investigated. A mathematical analysis of the model will appear elsewhere (Regalado & Sleeman 1997).

2. THE MATHEMATICAL MODEL

(*a*) *Cytoskeleton mechanical equation*

The cytoplasm is permeated by an organized fibrous network, the cytoskeleton, in which organelles are embedded and which regulates their movement (Bray 1992). While this is more or less accepted to be also the case in fungal cells (see, for example, McKerracher & Heath 1986, 1987; Heath 1995 and the references therein), the controversy is mainly centred in the organization, nature and composition of such a network. Nevertheless, we can imagine the cytoskeleton as an interconnected lattice of microtubules, actin filaments and associated proteins, which can be characterized as a fluid with viscous and elastic properties: elastic forces are a consequence of the proteic nature of individual filaments and their crosslinking; viscous properties arise because of steric impediments to the free diffusion of filaments (Pollard & Cooper 1986; Janmey *et al.* 1988, 1991; Luby-Phelps 1994). The cytoskeleton is involved in the motion of many organelles (McKerracher & Heath 1987; Heath 1995). Consequently, viscous and elastic forces are likely to affect the transport dynamics within the hyphal interior. Since vesicles are the most abundant organelles in the apical tip, it is likely that their motion is also affected by such forces. Because of its elastic properties, the cytoskeleton will also respond to cytoplasmic contractions accordingly (Heath 1995 and the references therein).

The mechanical properties of the cytoskeleton can be effectively described using elasticity theory (Timoshenko & Goodier 1970). Consider a one-dimensional cytoskeletal filament (or a one-dimensional section of the cytoskeleton) of length L at rest. Under deformation its length is modified to L_d and we measure deformation in terms of the non-dimensional quantity $\varepsilon = (L_\mathrm{d} - L)/L$, known as the strain. Hence if $L_\mathrm{d} = L$, then no deformation has taken place and $\varepsilon = 0$; while if $\varepsilon < 0$ ($\varepsilon > 0$) the filament is under compression (dilation). When dealing with objects of more than one dimension it is convenient to define the deformation of a point in the material relative to its position at rest, via the displacement vector $\boldsymbol{u}(\boldsymbol{r}, t)$. Thus a point initially at position $\boldsymbol{r} = x\hat{\boldsymbol{i}} + y\hat{\boldsymbol{j}} + z\hat{\boldsymbol{k}}$ is deformed (displaced) to $\boldsymbol{r} + \boldsymbol{u}$ at time t (with $\hat{\boldsymbol{i}}$, $\hat{\boldsymbol{j}}$ and $\hat{\boldsymbol{k}}$ being the unit vectors in the directions x, y and z, respectively). Accordingly, one can show that the strain will adopt a tensorial character (denoted by the superscript $\tilde{}$) and that it can be written in terms of $\boldsymbol{u}$ as

$$\tilde{\varepsilon} = \tfrac{1}{2}(\nabla \boldsymbol{u} + \nabla \boldsymbol{u}^{\mathrm{T}}). \tag{1}$$

In general the strain tensor can be written (Prager 1961)

$$\tilde{\varepsilon} = \begin{bmatrix} \varepsilon_{xx} & \varepsilon_{xy} & \varepsilon_{xz} \\ \varepsilon_{yx} & \varepsilon_{yy} & \varepsilon_{yz} \\ \varepsilon_{zx} & \varepsilon_{zy} & \varepsilon_{zz} \end{bmatrix},$$

where ε_{ij} ($= \varepsilon_{ji}$, $i \neq j$) are the components of strain, which uniquely define $\tilde{\varepsilon}$.

If we assume the different mechanical forces acting in the cytoskeleton to be in equilibrium (i.e. inertial forces are negligible), we can write according to Newton's second law

$$m\frac{\partial^2 \boldsymbol{u}}{\partial t^2} = \text{sum of forces} \equiv \text{viscous} + \text{elastic forces} = \boldsymbol{0}. \tag{2}$$

where m is the cytoskeleton density in a unit volume and $(\partial^2 \boldsymbol{u}/\partial t^2)$ is the acceleration of the network of filaments. General textbooks on continuum mechanics (Timoshenko & Goodier 1970; Landau & Lifshitz 1986) give the form of the different visco and elastic forces in equation (2). By assuming that the cytoskeleton is isotropic (i.e. its physical properties do not vary with direction) we can write

$$\boldsymbol{0} = \nabla \cdot \{[\eta\tilde{\varepsilon}_t + \xi\theta_t\tilde{I}] + E'[\tilde{\varepsilon} + \nu'\theta\tilde{I}]\}, \tag{3}$$
$$\underset{\text{viscous}}{\qquad\qquad} \underset{\text{elastic}}{\qquad\qquad}$$

with

$$E' = E/(1+\nu), \quad \nu' = \nu/(1-2\nu).$$

The constants η, ξ and E, ν are, respectively, viscous and elastic parameters, that is η is the shear viscosity, ξ the bulk viscosity, E the Young's modulus and ν denotes the Poisson ratio. As above, $\tilde{\varepsilon}$ is the strain tensor, and $\theta(= \nabla \cdot \boldsymbol{u})$ is the dilation; $\tilde{I}$ is the unit tensor,

$$\tilde{I} = \begin{bmatrix} 1 & 0 & 0 \\ 0 & 1 & 0 \\ 0 & 0 & 1 \end{bmatrix}.$$

(*b*) *Vesicle density conservation equation*

We describe changes in the spatio-temporal distribution of vesicles by means of a conservation equation of the form

$$\frac{\partial c}{\partial t} = -\nabla \cdot \boldsymbol{J}_{\text{ves}} = -\nabla \cdot \boldsymbol{J}_{\text{diff}} - \nabla \cdot \boldsymbol{J}_{\text{convec}}, \quad \text{in } \Omega, \tag{4}$$

where c denotes the number of vesicles per unit volume (vesicle density). $\boldsymbol{J}_{\text{diff}}$ and $\boldsymbol{J}_{\text{convec}}$ represent different contributions (discussed below) to the total flux of vesicles $\boldsymbol{J}_{\text{ves}}$, that is the number of vesicles crossing a unit area per unit time. The divergence, $\nabla\cdot$, of this quantity expresses the rate of loss of vesicles per unit volume. Ω is considered to be the spatial domain bounded by the site where vesicles are originated, i.e. the endoplasmic reticulum, and the site of vesicle delivery, i.e. the hyphal wall. Thus stated, equation (4) sets the rate of increase in vesicle density at a point, equal to the net flux of vesicles at that point, under the assumption that there is no net source of vesicles in Ω.

In order to distinguish phenomena due to increases in the overall vesicle density from those that are inherent to the postulated mechanisms, we assume that (unless otherwise stated) there is no change in the density of vesicles due to degradation or inclusion into the wall. More precisely, we consider that the formation or decay of vesicles is balanced by the number of vesicles that are accommodated into the wall. Thus we assume no-flux boundary conditions, i.e.

$$\boldsymbol{J}_{\text{ves}} \cdot \hat{\boldsymbol{n}} = 0, \quad \text{on } \partial\Omega,$$

where $\hat{\boldsymbol{n}}$ is the unit vector normal to a surface element and the boundary $\partial\Omega$ is physically placed at the hyphal wall. Since the hyphal tip is growing, we in reality have a moving boundary problem, with the boundary given by some $\partial\Omega(t)$. However, since tip growth is accompanied by cytoplasmic migration (McKerracher & Heath 1987), we may consider the boundary as being fixed with respect to an origin placed at the endoplasmic reticulum and hence $\partial\Omega(t)$ is invariant in time. We may also argue that, since the velocity of vesicles motion is much greater than the expansion rate of the tip (see § 1), small variations in $\partial\Omega$ are negligible, within the time scale considered here.

(*c*) *Mechanisms of vesicle motion*

(i) *Biased random motion* ($\boldsymbol{J}_{\text{diff}}$)

Heath & Kaminskyj (1989) found that the preferred longitudinal distribution of vesicles in the subapical peripheral cytoplasm of *Saprolegnia ferax* was coincident with the longitudinal alignment of actin cables in this zone (Heath & Kaminskyj 1989). Hoch *et al.* (1987) reported migration of vesicles along linear tracks in apical regions of *Uromyces* germlings. Other authors have also related cytoskeleton components to vesicle transport: Howard & Aist (1980) found that exposure of *Fusarium* hyphae to an antitubulin agent resulted in the disorganization of the Spitzenkörper (Howard & Aist 1977, 1980) and the alteration of the distribution pattern of wall vesicles (Howard & Aist 1980); Borett & Howard (1991) found actin filaments associated with the Spitzenkörper. Howard & Aist (1979) and Howard (1981) observed longitudinally oriented microtubules in subapical regions of hyphal tips of *Fusarium*. Occasionally these were observed in an apparent association with cytoplasmic vesicles (Howard 1981). However, Heath & Kaminskyj (1989) claim that such an association in *Saprolegnia* is coincidental and that the spatial distribution of microtubules within the hyphal tip and their typical length, tend to diminish their possible involvement in the transport of organelles (see also Heath *et al.* 1985). Finally, mutations in the actin gene of *Saccharomyces* have been demonstrated to lead to an abnormal distribution of actin filaments accompanied by an accumulation of secretory vesicles in the cytoplasm (Novick & Schekman 1979; Novick & Bolstein 1985).

We summarize the above observations in our model by assuming that vesicles move randomly, embedded in the network of filaments that form the cytoskeleton. We also assume that vesicle motion is solely affected by local variations in the surrounding environment (but for other kinds of dependences, see Othmer & Stevens 1997; Levine & Sleeman 1997; see also Cook 1995) and therefore the flux is given by:

$$\boldsymbol{J}_{\text{diff}} = -\nabla D c,$$

where D is the diffusivity. If stresses are applied to the cytoskeleton, these forces will be transmitted to the vesicles, which will consequently tend to move down a potential gradient, i.e. move from regions of high to low stress. This is modelled by assuming that the diffusion coefficient D is dependent on the elastic strain tensor $\tilde{\varepsilon}$, i.e. $\boldsymbol{J}_{\text{diff}} = -\nabla D(\tilde{\varepsilon})c$. The form of this dependence is taken to be (see § 4 *a* for other forms of $D(\tilde{\varepsilon})$)

$$\begin{aligned} D(\tilde{\varepsilon}) &= D_1|\tilde{\varepsilon}|^p \\ &= D_1(\varepsilon_{xx}^2 + 2\varepsilon_{xy}^2 + 2\varepsilon_{xz}^2 + 2\varepsilon_{yz}^2 + \varepsilon_{yy}^2 + \varepsilon_{zz}^2)^{p/2}, \end{aligned} \tag{5}$$

where ε_{ij} are, as above, the components of strain; p is some positive parameter which determines the shape of the power-law dependence in (5). D_1 is a proportionality constant. Equation (5) can be interpreted as stating that the diffusion of vesicles is facilitated (biased) according to the magnitude of the different contributions to the strain tensor by the components of strain in each direction (ε_{ij}). For example, under forces prevailing along the elongation direction (say the y-axis) filaments would tend to orientate longitudinally. Vesicle motion would accordingly be favoured along these lines of force (since according to (5) the leading contribution to the diffusivity would therefore come from ε_{yy}), parallel to the filaments, as has been observed (Howard 1983; Heath & Kaminskyj 1989). Equally, if the cytoskeletal network was disrupted, such that forces can no longer be transmitted, the above coupling would disappear ($p = 0$) and therefore the migration of vesicles along such linear tracks would be substituted by Brownian motion,

$D(\tilde{\varepsilon}) = D_1$. Herr & Heath (1982) and Hoch *et al.* (1987) observed a generalized increase in Brownian motion in *Uromyces* germlings treated with different antimicrotubule agents.

Notice also that from (5), $D(0) = 0$, which implies $c_t = 0$, (see (4)). It is expected that an applied deformation would relax over time. Therefore a stationary vesicle distribution will be achieved once the applied deformation has relaxed.

(ii) *Motion of vesicles result as a direct interaction with cytoskeleton filaments* ($\boldsymbol{J}_{\text{convec}}$)

The above discussed mechanism does not exclude the possibility of contact between vesicles and filaments. However, in its formulation it is implicit that such an association is not the ultimate cause for vesicle migration. A direct interaction between vesicles and cytoskeleton components, acting as (representing) the motive force for vesicle migration, cannot in principle be discarded. However, experimental observations showing the existence of such active transport of vesicles or a close association between vesicles and cytoskeleton filaments in fungal cells are inconclusive (Howard 1981; Heath *et al.* 1985; Vargas *et al.* 1993). The low vesicle–microtubule interaction frequencies observed in *Saprolegnia* (Heath *et al.* 1985; Heath & Kaminskyj 1989) may be due to a low affinity binding between vesicles and microtubules. However, it is difficult to reconcile how a weak interaction between both could transmit forces sufficient for vesicle movement, since the cytoplasmic streaming or simple Brownian motion would tend to disrupt such interactions. Some authors have suggested that sporadic observations, such as the existence of lines of vesicles in subapical regions of the cytoplasm of *Neurospora crassa* (Trinci & Collinge 1973) and *Volvariella volvacea* (Tanaka & Chang 1972), may be indicative of the existence of an intimate contact between filaments and vesicles. Additionally, Howard (1983) found several types of vesicles closely associated with microtubules arranged in a track-like configuration.

Despite the lack of experimental evidence to support an active motion of vesicles via interactions with cytoskeletal components, we explore its relevance in our model. There is as yet no postulated mechanism by which fungal cytoskeletal components would mediate organelle movement along them. Most of the related work comes from other organisms, principally microtubule-mediated vesicle transport in the axoplasm of the squid giant axon (see, for example, Weiss 1986). Since the force-generating mechanism is unknown, we hypothesize a mechanism of motion based on the following observations (see Weiss 1986 for a review). (i) The attachment and traction of a vesicle can deform a filament elastically (Vale *et al.* 1985; Weiss 1986). (ii) Organelle movement can take place along single filaments (microtubules) (Schnapp *et al.* 1985); thus vesicles may be pulled forward by the local deformation of the cytoskeleton filaments; hence, the velocity of deformation is $\boldsymbol{v}_{\text{convec}} = \partial \boldsymbol{u}(\boldsymbol{r}, t)/\partial t$. Other forms of such advective velocity can be proposed. Most of the results obtained here are, however, independent of the detailed form of $\boldsymbol{v}_{\text{convec}}$. (iii) Experiments with axoplasm extruded from squid giant axons show that the number of particles transported is proportional to the number in suspension (Vale *et al.* 1985; Weiss 1986); the number of vesicles transported per unit of time is therefore proportional to c times such velocity of deformation, i.e.

$$\boldsymbol{J}_{\text{convec}} = D_2 c \frac{\partial \boldsymbol{u}(\boldsymbol{r}, t)}{\partial t}. \tag{6}$$

(iv) Axoplasmic organelles appear to have multiple binding sites and when attached to more than one filament their velocity of movement is diminished (Vale *et al.* 1985); we model this by making $\boldsymbol{J}_{\text{convec}}$ inversely proportional to the filament density m. However, we assume $m(\boldsymbol{r}, t)$ to be constant and therefore rescaled to D_2. A term of the form of (6) has been considered by Murray & Oster (1984*a*) in a model for cell traction during mesenchymal morphogenesis.

The main hypotheses considered in the model are schematically depicted in figure 1*b*. In summary, the model comprises the following system

$$\left.\begin{aligned} c_t &= D_1 \nabla \cdot (\nabla |\tilde{\varepsilon}|^p c) - D_2 \nabla \cdot (u_t c), \\ \mathbf{0} &= \nabla \cdot \{[\eta \tilde{\varepsilon}_t + \xi \theta_t \tilde{I}] + E'[\tilde{\varepsilon} + \nu' \theta \tilde{I}]\}, \end{aligned}\right\} \tag{7}$$

together with null boundary conditions

$$-(D_1 \nabla |\tilde{\varepsilon}|^p c - D_2 u_t c) \cdot \hat{\boldsymbol{n}} = 0, \quad \nabla \cdot \tilde{\varepsilon} = \mathbf{0}, \quad \text{on } \partial\Omega. \tag{8}$$

3. RESULTS

We investigate the dynamical behaviour of numerical solutions of system (7), (8), in one and two space dimensions. An initial deformation is applied to the cytoskeleton. The spatio-temporal evolution of an initial distribution of wall vesicles, subjected to viscoelastic forces, is then followed under two sets of assumptions: model 1, 3, where vesicles are simply passively driven by viscoelastic forces ($D_2 = 0$) and, model 2, where vesicles are also actively dragged along filaments ($D_2 \neq 0$).

(*a*) *Model 1*

It is assumed that there are no mechanical tractions between vesicles and cytoskeleton. Vesicles are simply biased in their motion by cytoskeletal forces ($D_2 = 0$). One-dimensional model.

Two main types of generic behaviour in the dynamics of vesicle motion were observed: either an initial spatially uniform population of vesicles transiently clustered in a localized region before collapsing to a spatially uniform distribution (e.g. figure 2), or such an accumulation peak remained stationary over time (e.g. figure 3). We will refer to the former as collapse and to the latter as aggregation. Whether

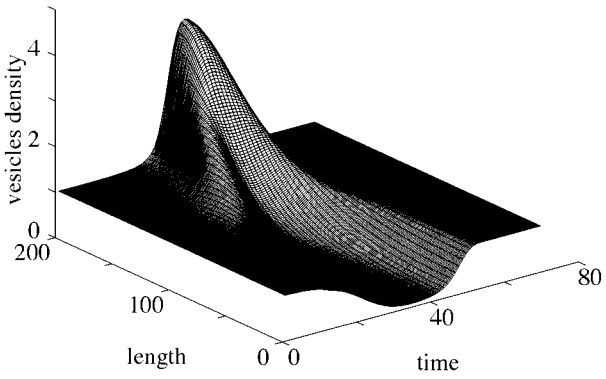

Figure 2. An example of vesicle collapse in one dimension from an initially homogeneous vesicle distribution, $c_0 = 1$. An initial deformation of the form $2 + \cos \pi x$ was applied to the cytoskeleton. The displacement at both ends of the interval, Golgi side ($u^{(0)}$) and wall apex ($u^{(1)}$), is taken to be of the form: $u^{(1)} - u^{(0)} = 2$. The parameter values used in the simulation are: $p = 4$; $\hat{\mu} = (E'(1 + \nu')/\eta + \xi) = 1$; $D_1 = 1$; $D_2 = 0$.

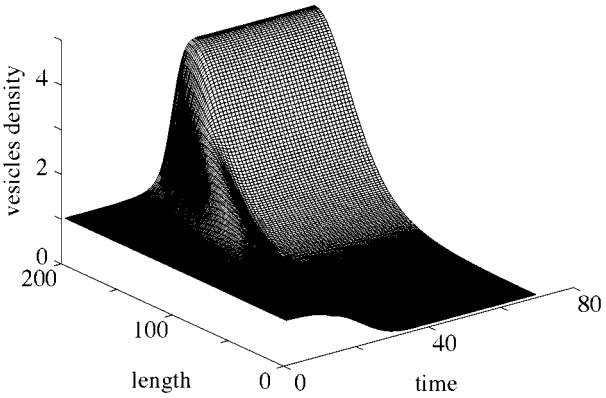

Figure 3. An example of vesicle aggregation in one dimension. A deformation of the form $2 + \cos \pi x$ was initially applied to the cytoskeleton. The displacement at both ends of the interval, Golgi side ($u^{(0)}$) and wall apex ($u^{(1)}$), is taken to be of the form: $u^{(1)} - u^{(0)} = 2\mathrm{e}^{-t}$. The parameter values used in the simulation are: $p = 4$; $\hat{\mu} = (E'(1 + \nu')/\eta + \xi) = 1$; $D_1 = c_0 = 1$; $D_2 = 0$.

vesicles will eventually collapse or aggregate does not depend upon a particular choice of parameter values but, upon the form of both the displacement at the hyphal tip wall and Golgi side (compare figures 2 and 3). Different choices of, e.g. viscous and elastic parameters, will only affect the shape and positioning of the aggregation and collapse peaks (see below), but do not decide whether one or the other will take place.

An accumulation of vesicles or Spitzenkörper, associated with growth, was described initially by Brunswik (1924), although its precise mechanism of formation has since remained unknown. The results presented here suggest that vesicles accumulate as a consequence of cytoskeletal forces modulating their random motion. The capacity for disorganizing (collapse of) such aggregation centres under certain circumstances seems also desirable, since structural changes in the organization of the Spitzenkörper are directly involved in growth and branching. Exam-

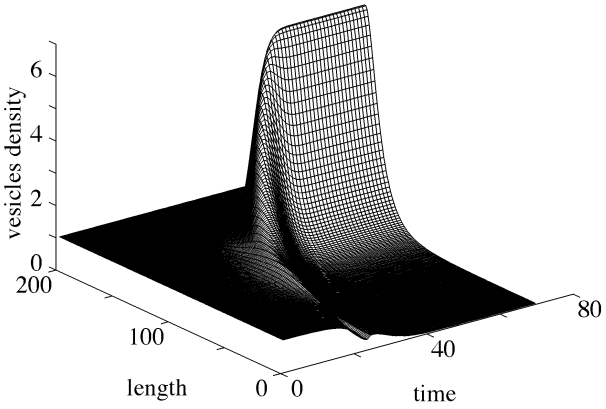

Figure 4. An example of vesicle aggregation in one dimension. The aggregation peak can be moved by changing the initial deformation, $1 + \cos \pi x$. Compare with figure 3. The displacement at both ends of the interval, Golgi side ($u^{(0)}$) and wall apex ($u^{(1)}$), is taken to be of the form: $u^{(1)} - u^{(0)} = \mathrm{e}^{-t}$. The parameter values used in the simulation are: $p = 4$; $\hat{\mu} = (E'(1 + \nu')/\eta + \xi) = 1$; $D_1 = c_0 = 1$; $D_2 = 0$.

ples that illustrate this fact are: in hypha that have stopped growing, the Spitzenkörper appears disorganized; perturbations of a growing hypha, for example by mechanical forces, lead to the disappearance of the Spitzenkörper (Girbardt 1957; López-Franco 1992; López-Franco & Bracker 1996); the dynamical reorganization of the Spitzenkörper in association with apical branching has recently been described (Reynaga-Peña *et al.* 1995; see below). The model presented here is capable of reproducing conditions where such collapse may take place.

The position of the Spitzenkörper is responsible for the shaping of the tip and its vectorial growth (Bartnicki-Garcia *et al.* 1989). A mechanism is therefore required whereby the position of the aggregation centre can change. In addition, the morphology of the Spitzenkörper varies between fungi (see Gow 1995, figure 13.1; López-Franco & Bracker 1996). In figures 2–4 vesicles are collected further back from the tip ($x = 0$ side) and accumulation happens to be close to the tip apex. However, such accumulation peaks can be moved both in time and space by changing the form of the initial deformation (compare figures 3 and 4) or the value of p (result not shown). However, the shape and size of the initial distribution of vesicles does not modify the final outcome of the aggregation and collapse dynamics.

To date the only mechanism proposed to explain the initiation of branching in hyphae relies on an accumulation of vesicles, due to either the existence of physical barriers along the hyphal tube (septa), or an imbalance between the rate of incorporation of vesicles into the wall and their rate of supply by Golgi bodies (Trinci 1974, 1978). In order to investigate the possibility of branching by means of an increase in the overall number of vesicles, we impose different boundary conditions at both ends of the interval, such that the vesicle density does not remain conserved. We therefore consider the influx

PHILOSOPHICAL TRANSACTIONS OF THE ROYAL SOCIETY B BIOLOGICAL SCIENCES

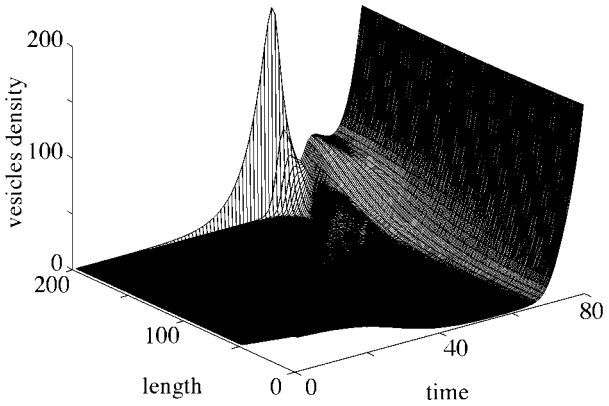

Figure 5. The vesicle population grows unbounded if the vesicle density is not conserved across the boundary: the influx at the Golgi side ($\boldsymbol{J}_{\text{ves}} = 5$ at $x = 0$), was considered to be double the efflux of vesicles at the wall apex ($\boldsymbol{J}_{\text{ves}} = -10$). The initial deformation applied to the cytoskeleton is of the form $1 + \cos \pi x$. Other parameter values are: $u^{(1)} - u^{(0)} = 1$; $p = 4$; $\hat{\mu} = (E'(1 + \nu')/\eta + \xi) = 1$; $D_1 = c_0 = 1$; $D_2 = 0$.

of vesicles at one end (endoplasmic side) to be double the efflux of vesicles at the other end (wall apex) ($\boldsymbol{J}_{\text{ves}} = -10$ at $x = 1$ and $\boldsymbol{J}_{\text{ves}} = 5$ at $x = 0$). Figure 5 shows the predicted outcome under these circumstances. After an initial transient aggregation the vesicle density collapses and it is followed by an unbounded growth, but no breaking of symmetry of the aggregation peak is observed. This suggests that the possibility of branching initiation by a differential flux of vesicles at their site of formation and their rate of incorporation to the hyphal wall, is not tenable.

(*b*) *Model 2*

Vesicles are not solely diffusion driven but are also dragged by the cytoskeleton ($D_2 \neq 0$). One-dimensional model.

We investigate the effect of an assumed dragging force acting on the vesicle population by increasing D_2 (figures 6–8). In the case of positive drift ($D_2 > 0$) vesicles accumulate from the endoplasmic side ($x = 0$ side) and a backward accumulation of vesicles occurs, with the aggregation peak moving towards the right (figures 6 and 7). When the drift is negative (figure 8) the opposite happens and vesicles accumulate only from the right-hand side. As the vesicles aggregate they advance. The aggregation centre then displaces as a whole towards one of the ends.

Small clusters of vesicles, or satellite Spitzenkörper, moving as a whole, have recently been reported by López-Franco *et al.* (1995). After an initial aggregation phase the satellites migrate along the periphery of the hypha and coalesce with the Spitzenkörper (López-Franco *et al.* 1995). The Spitzenkörper itself is not static either but can displace also (Bartnicki-Garcia *et al.* 1989; López-Franco *et al.* 1995). The origin of formation of satellites is conjectured to be similar to that of the

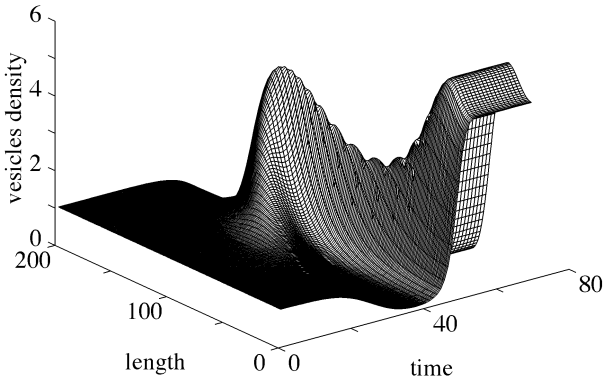

Figure 6. Convective forces can shift the aggregation peak as a whole. Same parameter values as in figure 3 with $D_2 = 5$.

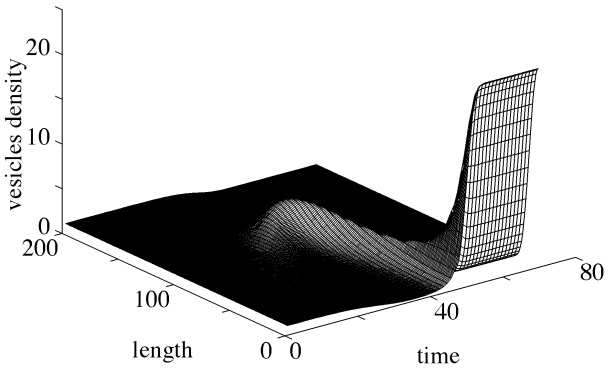

Figure 7. Convective forces can shift the aggregation peak as a whole. Same parameter values as in figure 3 with $D_2 = 10$.

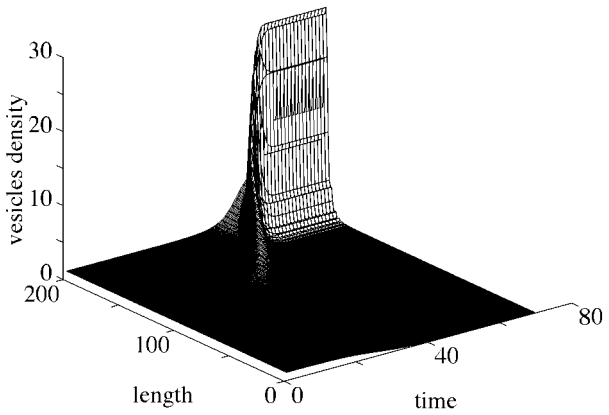

Figure 8. Convective forces can shift the aggregation peak as a whole. Same parameter values as in figure 3 with $D_2 = -2$.

Spitzenkörper (López-Franco *et al.* 1995). The results presented here favour this last hypothesis: a diffusion-driven mechanism may lead initially to the formation of discrete cluster of vesicles (plaque and growth stages in López-Franco's terminology). Subsequently, the existence of convective forces pulling vesicles forward, would favour the migration *en masse* of such clusters (migratory stage, according to López-Franco). Such a mechanism appears to indicate the need for an intimate contact between vesicles and cytoplasmic filaments. Associations of migrating

PHILOSOPHICAL TRANSACTIONS OF THE ROYAL SOCIETY B BIOLOGICAL SCIENCES

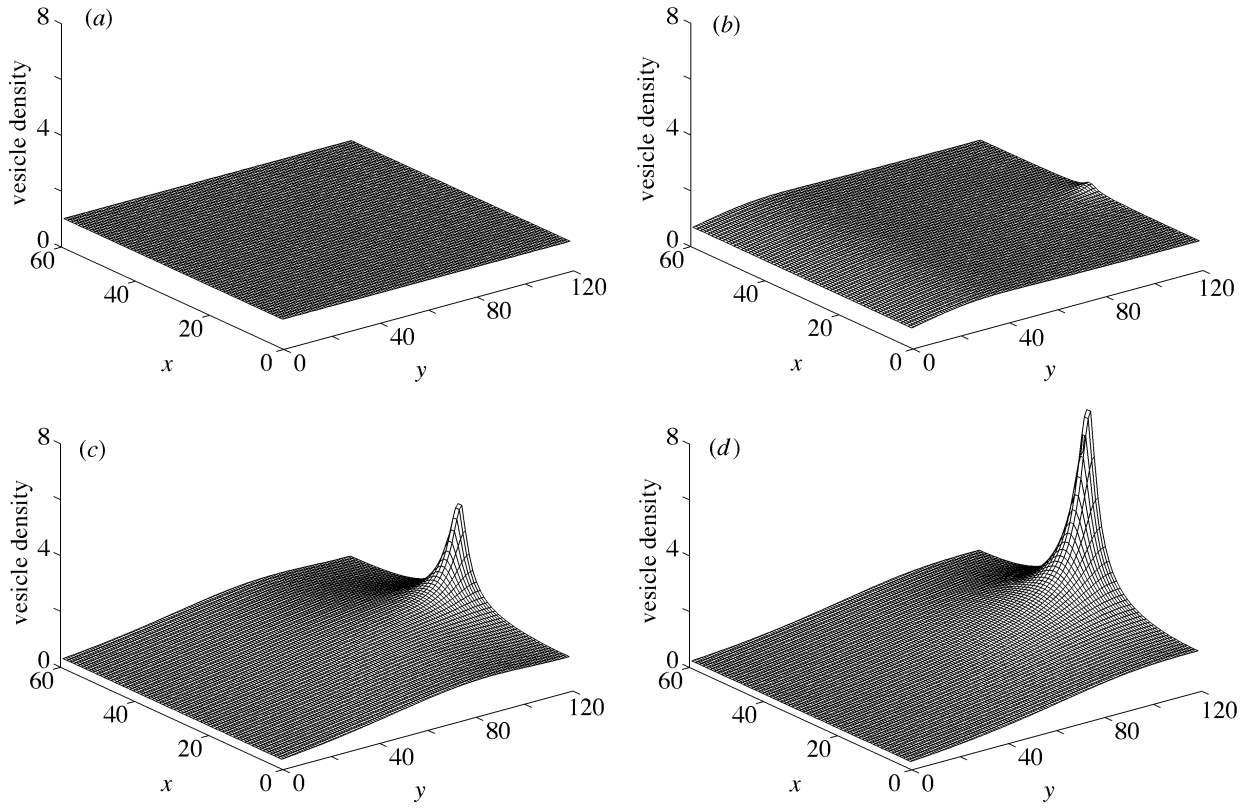

Figure 9. An example of vesicle aggregation in two dimensions, from an initially homogeneous vesicle distribution, $c_0(x, y) = 1$. The parameter values chosen in the simulation are: $\hat{\xi} = \xi + \frac{4}{3}\eta = 1$; $\Pi = (E'(\nu' + 1)/\hat{\xi}) = 100$; $p = D_1 = 1$; $D_2 = 0$. The displacement normal (perpendicular) to the boundary is of the form $\boldsymbol{u} \cdot \hat{\boldsymbol{n}} = 1$. (*a*) Time, $t = 0.000$ (arbitrary units); (*b*) $t = 0.002$; (*c*) $t = 0.202$; (*d*) $t = 0.402$.

satellites with cytoplasmic filaments departing from the Spitzenkörper were reported by López-Franco *et al.* (1995). As the satellite approached the vicinity of the Spitzenkörper such filaments seem to bend (López-Franco *et al.* 1995).

(*c*) *Model 3*

The two-dimensional model and branching.

It is not only desirable to extend the above results to more than one dimension because of their greater realism, but because certain phenomena, such as branching, are more accurately represented in more than one dimension. Figures 9 and 10 show a time sequence during an aggregation and collapse event, respectively. Reynaga-Peña *et al.* 1995, described the sequence of events leading to apical branching in a mutant of *Aspergillus niger*: after a cytoplasmic contraction the Spitzenkörper 'disappeared' from view, accompanied by a reduction in hyphal growth rate and followed by a period of inactivity, after which the Spitzenkörper resumed as two new aggregation centres. From each of them an apical branch developed (Reynaga-Peña *et al.* 1995). Figure 11 shows a time sequence where, after applying an initial deformation to the cytoskeleton, an initial single vesicle cluster (figure 11*a*) collapses (figures 11*b*, *c*) to form two distinct aggregation centres (figures 11*d*, *e*), suggesting that during the period of low activity described by Reynaga-Peña *et al.* (1995), the Spitzenkörper may have in fact disorganized (collapsed). These results also contribute to validate the mechanism of Spitzenkörper organization proposed here, and to provide an understanding of how apical branch initiation may occur, without resorting to the existence of physical barriers (septae) (Prosser & Trinci 1979; Yang *et al.* 1992), or to an increase in the overall vesicle density (Trinci 1974, 1978; see above).

4. CONCLUSIONS AND DISCUSSION

Since its first citation by Brunswik in 1924, evidence has accumulated about the involvement of the Spitzenkörper in the shaping of the hyphal tip, tip polarization and initiation of branching. All of these processes are central to fungal morphogenesis, hence the interest for understanding the origin of formation of the Spitzenkörper and its dynamics. In addition, there is experimental evidence involving the hyphal cytoskeleton in the motion of vesicles and in the organization of the Spitzenkörper. However, experimental techniques have so far failed to reveal either a mechanism for wall vesicle motion or Spitzenkörper formation. In searching for a mechanism for the origin of the Spitzenkörper, the question arises as to whether the Spitzenkörper plays an active role in the recruitment of wall vesicles, or whether this appears as a consequence of the vesicles motion mechanism itself. The former hypothesis becomes tautological when one tries to explain the formation of a Spitzenkörper

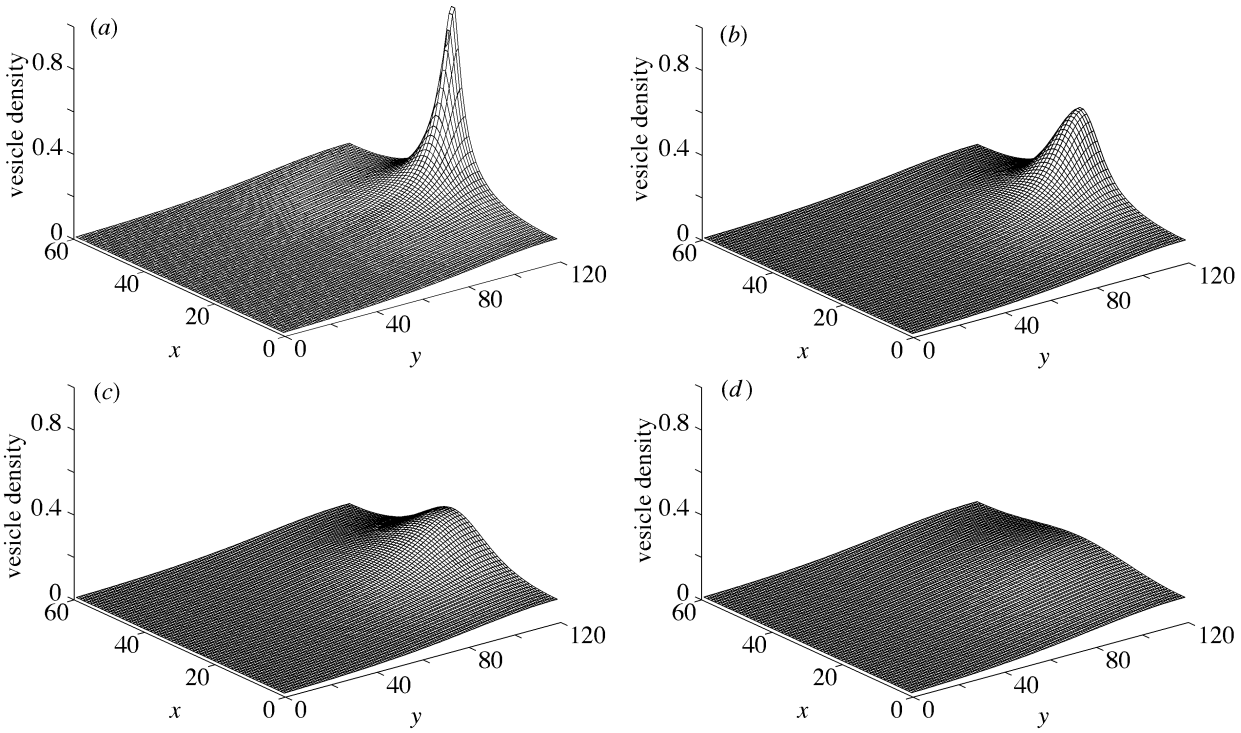

Figure 10. An example of vesicle collapse in two dimensions, from an initial vesicle distribution of the form $c_0(x, y) = (\pi^4 \cos^2 \pi x + \pi^4 \sinh^2 \pi(1-y)+1)^{-1/2}$. (*a*) Time, $t = 0.000$ (arbitrary units); (*b*) $t = 0.055$; (*c*) $t = 0.105$; (*d*) $t = 0.205$. Parameter values are as in figure 9. with a normal displacement at the boundary of the form $\boldsymbol{u} \cdot \hat{\boldsymbol{n}} = 1 + 100t$.

where initially there was no such structure; the latter requires reconciliation of how local events, such as the motion of single vesicles, can lead to aggregation, an event which appears to require a long-range orchestration. How these 'microscopic' events (vesicular level) are then translated into 'macroscopic' phenomena, such as satellite and Spitzenkörper dynamical organization, then needs explanation. We have succeeded in providing a mechanism for this to take place based on first principles, such as Brownian motion and viscoelastic properties. In fact, both seem unavoidable, the former because of the microscopic size of the vesicles, and the latter because of the filamentous nature of the cytoskeleton. We show that a mechanism of motion solely based on these two principles would lead to either aggregation or collapse of vesicles. In addition, if a certain size of the vesicle population is assumed to remain attached to the cytoskeleton and to use this as a motor mechanism, we show this may lead to the migration *en masse* of vesicle clusters or satellite Spitzenkörper. We also find situations where an established aggregation peak can collapse to reform as two distinct organizing centres, in accordance with what has recently been described as the sequence of events leading to apical branching. These results reinforce the validity of the mechanism proposed here; however, only more experimental evidence will decide whether this or other mechanisms are in fact taking place in the interior of the hypha. In saying this, data regarding microscopic features of vesicle motion, such as velocity, turning angle distributions or characteristics of the path followed by vesicles, would be beneficial in further discerning the applicability of the model presented here.

(*a*) *Anisotropy and other forms of the strain-dependent diffusion coefficient*

The form of the diffusion coefficient $D(\tilde{\varepsilon})$ in (5) is only one of a variety of possibilities. $D(\tilde{\varepsilon})$ is chosen to depend on the magnitude of $\tilde{\varepsilon}$ and directionality follows from the gradient of vesicles—which is proportional to the strain tensor, $\nabla|\tilde{\varepsilon}|c$, such that vesicle motion will be primarily favoured along the direction of highest strain or axis of deformation. Since it is predicted that, as a consequence of the deformation, cytoskeleton filaments will distribute preferably along such an axis, vesicle motion will also be facilitated along that direction. However, filament orientation is not explicitly described in the model, although there is evidence to suggest a preferred orientation of cytoskeleton filaments in hyphal tips. For example, microtubules in hyphal tips of *Fusarium* are oriented longitudinally (see section on biased random motion). In order to model this phenomena, other forms of the diffusion tensor may be used. For example, when the local filament orientation distribution is specified, Cook (1995) showed that the diffusion coefficient $D(\tilde{\varepsilon})$ is of the form

$$D(\tilde{\varepsilon}) = \tfrac{1}{4} D_1 \begin{bmatrix} 2 + \varepsilon_{xx} - \varepsilon_{yy} & 2\varepsilon_{xy} \\ 2\varepsilon_{xy} & 2 + \varepsilon_{yy} - \varepsilon_{xx} \end{bmatrix}, \qquad (9)$$

where ε_{ij} are, as before, the strain components in the corresponding directions. The above form of the diffusion coefficient predicts that diffusion is proportional to the degree of filament alignment due to strain, i.e. diffusion is small unless filaments are aligned and stretched. The diffusion coefficient specified by (9) is reducible to a class of diffusion matrices

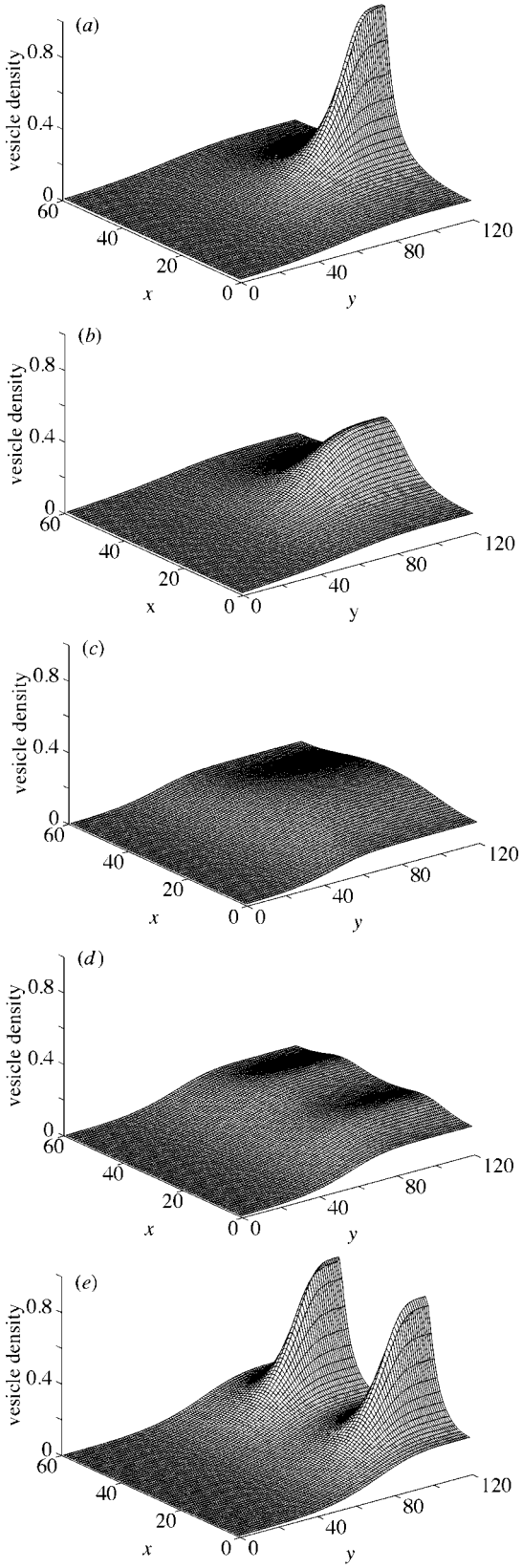

Figure 11. An initial vesicle cluster (a), collapses (b, c), before reorganizing as two new aggregation centres (d, e), when an initial deformation of the form $\frac{1}{2}(x^2 + y^2)$ is applied to the cytoskeleton. The time sequence shown is as follows: (a) Time, $t = 0.000$ (arbitrary units); (b) $t = 0.015$; (c) $t = 0.120$; (d) $t = 0.240$; (e) $t = 0.960$. The parameter values chosen in the simulation are: $\hat{\xi} = \xi + \frac{4}{3}\eta = 1$; $\Pi = (E'(\nu' + 1)/\hat{\xi}) = 10$; $c_0 = p = D_1 = 1$; $D_2 = 0$. The displacement normal (perpendicular) to the boundary is of the form $\boldsymbol{u} \cdot \hat{\boldsymbol{n}} = 1 + \mathrm{e}^{-0.5t}$.

of the form (Cook 1995)

$$D = \begin{bmatrix} f(\varepsilon) & 0 \\ 0 & f(-\varepsilon) \end{bmatrix}, \tag{10}$$

where $f(\pm\varepsilon)$ is a measure of the 'strength' of diffusion in the x- and y-directions, respectively. ε measures the degree of anisotropy which varies between $+1$, complete filament alignment in the y-direction, and -1, complete alignment in the x-direction (with $\varepsilon = 0$ reflecting isotropy). For example, (9) corresponds to $f(\varepsilon) = \frac{1}{2}(1 - \varepsilon)$. The diffusion coefficient specified by (9), and more generally by (10), would therefore permit us to include anisotropy and filament alignment in the equation governing vesicle motion. These are considerations which deserve further investigation.

The authors thank Dr J. W. Crawford for his comments on the manuscript. This work is funded by the Scottish Office Agriculture and Fisheries Department.

REFERENCES

Andrews, J. H. 1995 Fungi and the evolution of growth form. *Can. J. Botany* **73**, 1206–1212.

Bartnicki-Garcia, S., Bartnicki, D. D., Gierz, G., López-Franco, R. & Bracker, C. E. 1995 Evidence that the Spitzenkörper behavior determines the shape of a fungal hypha: a test of the hyphoid model. *Exp. Mycol.* **19**, 153–159.

Bartnicki-Garcia, S., Hergert, F. & Gierz, G. 1989 Computer simulation of fungal morphogenesis and the mathematical basis for hyphal (tip) growth. *Protoplasma* **153**, 46–57.

Bonnett Jr, H. T. & Newcomb, E. H. 1966 Coated vesicles and other cytoplasmic components of growing root hairs of radish. *Protoplasma* **62**, 59–75.

Borett, T. M. & Howard, R. J. 1991 Ultrastructural immunolocalization of actin in fungus. *Protoplasma* **163**, 199–202.

Bray, D. 1992 *Cell movements*. New York: Garland.

Brunswik, H. 1924 Untersuchungen ber Geschlechts–und Kernverhältnisse bei der *Hymenomyzetengattung coprinus*. In *Botanische abhandlungen* (ed. K. Goebel), pp. 1–152. Jena, Germany: Gustav Fischer.

Carlile, M. J. 1995 The success of the hypha and the mycelium. In *The growing fungus* (ed. N. A. R. Gow & G. M. Gadd), pp. 3–19. London: Chapman & Hall.

Collinge, A. J. & Trinci, A. P. J. 1974 Hyphal tips of wild type and spreading colonial mutants of *Neurospora crassa*. *Arch. Microbiol.* **99**, 353–368.

Cook, J. 1995 Mathematical models for dermal wound healing: wound contraction and scar formation. Ph.D. Thesis, University of Washington, Seattle.

Girbardt, M. 1957 Der Spitzenkörper von *Polystictus versicolor*. *Planta* **50**, 47–59.

Girbardt, M. 1969 Die ultrastruktur der apikalregion von pilzhyphen. *Protoplasma* **67**, 413–441.

Gow, N. A. R. 1995 Tip growth and polarity. In *The growing fungus* (ed. N. A. R. Gow & G. M. Gadd), pp. 277–299. London: Chapman & Hall.

Grove, S. N. 1978 The cytology of hyphal tip growth. In *The filamentous fungi. Developmental mycology*, vol. 3 (ed. J. E. Smith & D. R. Berry), pp. 28–50. London: Arnold.

PHILOSOPHICAL TRANSACTIONS OF THE ROYAL SOCIETY B BIOLOGICAL SCIENCES

Grove, S. N. & Bracker, C. E. 1970 Protoplasmic organization of hyphal tips among fungi: vesicles and Spitzenkörper. *J. Bacteriol.* **104**, 989–1009.

Heath, I. B. 1995 The cytoskeleton. In *The growing fungus* (ed. N. A. R. Gow & G. M. Gadd), pp. 99–134. London: Chapman & Hall.

Heath, I. B. & Kaminskyj, S. G. W. 1989 The organization of tip-growth-related organelles and microtubules revealed by quantitative analysis of freeze-substituted oomycete hyphae. *J. Cell Sci.* **1993**, 41–52.

Heath, I. B., Rethoret, K., Arsenhault, A. L. & Ottensmeyer, S. P. 1985 Improved preservation of the form and contents of wall vesicles and the Golgi apparatus in freeze substituted hyphae of *Saprolegnia*. *Protoplasma* **128**, 81–93.

Herr, F. B. & Heath, M. C. 1982 The effects of antimicrotubule agents on organelle positioning in the cowpea rust fungus, *Uromyces phaseoli* var *vignae*. *Exp. Mycol.* **6**, 15–24.

Hoch, H. C. & Tucker, B. E. & Staples, R. C. 1987 An intact microtubule cytoskeleton is necessary for mediation of the signal for cell differentiation in *Uromyces*. *Eur. J. Cell Biol.* **45**, 209–218.

Howard, R. J. 1981 Ultrastructural analysis of hyphal tip cell growth in fungi: Spitzenkörper, cytoskeleton and endomembranes after freeze-substitution. *J. Cell Sci.* **48**, 89–103.

Howard, R. J. 1983 Cytoplasmic transport in hyphae of *Gilbertella*. *Mycol. Soc. Am. Newsletter* **34**, 24.

Howard, R. J. & Aist, J. R. 1977 Effects of MBC on hyphal tip organization, growth, and mitosis of *Fusarium acuminatum*, and their antagonism by D_2O. *Protoplasma* **92**, 195–210.

Howard, R. J. & Aist, J. R. 1979 Hyphal tip cell ultrastructure of the fungus *Fusarium*: improved preservation by free-substitution. *J. Ultrastructure Res.* **66**, 224–234.

Howard, R. J. & Aist, J. R. 1980 Cytoplasmic microtubules and fungal morphogenesis: ultrastructural effects of methyl benzimidazole-2-yl-carbamate determined by freeze-substitution of hyphal tip cells. *J. Cell Biol.* **87**, 55–64.

Janmey, P. A., Hvidt, S., Peetermans, J., Lamb, I., Ferry, J. D. & Stossel, T. P. 1988 Viscoelasticity of F-actin and F-actin/gelsolin complexes. *Biochemistry* **27**, 8218–8226.

Janmey, P. A., Eutenwer, U., Traub, P. & Schliwa, M. 1991 Viscoelastic properties of vimentin compared with other filamentous biopolymer networks. *J. Cell Biol.* **113**, 155–160.

Kaminskyj, S. G. W., Garrill, A. & Heath, I. B. 1992 The relation between turgor and tip growth in *Saprolegnia ferax*: turgor is necessary, but not sufficient to explain apical extension rates. *Exp. Mycol.* **16**, 64–75.

Koch, A. L. 1982 The shape of the hyphal tips of fungi. *J. Gen. Microbiol.* **128**, 947–951.

Landau, L. D. & Lifshitz, E. M. 1986 Theory of elasticity. In *Course of theoretical physics* (ed. E. M. Lifshitz, A. M. Kosevich & L. P. Pitaevskiĭ), vol. 3. Oxford: Pergamon.

Levine, H. A. & Sleeman, B. D. 1997 A system of reaction diffusion equation arising in the theory of reinforced random walks. *SIAM J. Appl. Math.* **57**, 683–730.

López-Franco, R. 1992 Organization and dynamics of the Spitzenkörper in growing hyphal tips. Ph.D. Thesis, Purdue University, W. Lafayette, IN.

López-Franco, R., Bartnicki-Garcia, S. & Bracker, C. E. 1994 Pulsed growth of fungal hyphal tips. *Proc. Natn. Acad. Sci. USA* **91**, 12 228–12 232.

López-Franco, R., Howard, R. J. & Bracker, C. E. 1995 Satellite Spitzenkörper in growing hyphal tips. *Protoplasma* **188**, 85–103.

López-Franco, R. & Bracker, C. E. 1996 Diversity and dynamics of the Spitzenkörper in growing hyphal tips of higher fungi. *Protoplasma* **195**, 90–111.

Luby-Phelps, K. 1994 Physical properties of cytoplasm. *Curr. Opin. Cell Biol.* **6**, 3–9.

McKerracher, L. J. & Heath, I. B. 1986 Comparison of polyethylene glycol and diethylene glycol disterate embedding methods for the preservation of fungal cytoskeletons. *J. Electron Microsc. Tech.* **4**, 347–360.

McKerracher, L. J. & Heath, I. B. 1987 Cytoplasmic migration and intracellular organelle movements during tip growth of fungal hyphae. *Exp. Mycol.* **11**, 79–100.

Money, N. P. 1990 Measurement of turgor pressure. *Exp. Mycol.* **14**, 416–425.

Money, N. P. & Harold, F. M. 1992 Extension of the water mold *Achila*: interplay of turgor and wall strength. *Proc. Natn. Acad. Sci. USA* **89**, 4245–4249.

Murray, J. D. & Oster, G. F. 1984*a* Cell traction models for generating pattern and form in morphogenesis. *J. Math. Biol.* **19**, 256–279.

Murray, J. D. & Oster, G. F. 1984*b* Generation of biological pattern and form. *IMA Jl Math. Appl. Med. Biol.* **1**, 51–75.

Murray, J. D., Oster, G. F. & Harris, A. K. 1983 A mechanical model for mesenchymal morphogenesis. *J. Math. Biol.* **17**, 125–129.

Novick, P. & Bolstein, D. 1985 Phenotypic analysis of temperature-sensitive yeast actin mutants. *Cell* **40**, 405–416.

Novick, P. & Schekman, R. 1979 Secretion and cell-surface growth are blocked in a temperature-sensitive mutant of *Saccharomyces cerevisiae*. *Proc. Natn. Acad. Sci. USA* **76**, 1858–1862.

Oster, G. F., Murray, J. D. & Harris, A. K. 1983 Mechanical aspecs of mesenchymal morphogenesis, *J. Embryol. Exp. Morphol.* **78**, 83–125.

Othmer, H. G. & Stevens, A. 1997 Aggregation, blow up and collapse: the ABC of taxis in reinforced random walks. *SIAM Jl Appl. Math.* **57**, 1044–1081.

Pollard, T. D. & Cooper, J. A. 1986 Actin and actin-binding proteins. A critical evaluation of mechanism and functions. *A. Rev. Biochem.* **55**, 987–1035.

Prager, W. 1961 Introduction to mechanics of continua. In *Introductions to higher mathematics*. Boston, MA: Ginn.

Prosser, J. I. & Trinci, A. P. J. 1979 A model for mycelial growth. *J. Gen. Microbiol.* **111**, 153–164.

Reynaga-Peña, C. G., Bracker, C. E. & Bartnicki-Garcia, S. 1995 Cytoplasmic contractions, Spitzenkörper behavior and apical branching in *Aspergillus niger*. In *Annual meeting of the Mycological Society of America.*

Schnapp, B. J., Vale, R. D., Sheetz, M. P. & Reese, T. S. 1985 Single microtubules from squid axoplasm support bidirectional movement of organelles. *Cell* **40**, 455–462.

Steer, M. W. & Steer, J. M. 1989 Pollen tube tip growth. Tansley review No. 16. *New Phytol.* **111**, 323–358.

Tanaka, K. & Chang, S. 1972 Cytoplasmic vesicles in the growing hyphae of the Basidiomicete, *Volvariella volvacea*. *J. Gen. Appl. Microbiol.* **18**, 165–179.

Timoshenko, S. P. & Goodier, J. N. 1970 Theory of elasticity. *Engineering societies monographs*, 3rd edn. New York: McGraw-Hill.

Trinci, A. P. J. 1971 Influence of the width of the peripheral growth zone on the radial growth of fungal colonies on solid media. *J. Gen. Microbiol.* **67**, 325–344.

Trinci, A. P. J. 1974 A study of the kinetics of hyphal

PHILOSOPHICAL TRANSACTIONS OF THE ROYAL SOCIETY B BIOLOGICAL SCIENCES

extension and branch initiation of fungal mycelia. *J. Gen. Microbiol.* **81**, 225–236.

Trinci, A. P. J. 1978 The duplication cycle and vegetative development in moulds. In *The filamentous fungi*, vol. 3 (ed. J. E. Smith & D. R. Berry), pp. 132–163. London: Arnold.

Trinci, A. P. J. & Collinge, A. J. 1973 Structure and plugging of septa of wild type and spreading colonial mutants of *Neurospora crassa*. *Arch. Mikrobiol.* **91**, 355–364.

Vale, R. D., Schnapp, B. J., Reese, T. S. & Sheetz, M. P. 1985 Movement of organelles along filaments dissociated from the axoplasm of the squid giant axon. *Cell* **40**, 449–454.

Vargas, M. M., Aronson, J. M. & Roberson, R. W. 1993 The cytoplasmic organization of hyphal tip cells in the fungus *Allomyces macrogynus*. *Protoplasma* **176**, 43–52.

Weiss, D. G. 1986 Visualization of the living cytoskeleton by video-enhanced microscopy and digital image processing. *J. Cell Sci. Suppl.* **5**, 1–15.

Yang, H., King, R., Reichl, U. & Gilles, E. D. 1992 Mathematical model for apical growth, septation, and branching of mycelial microorganisms. *Biotech. Bioengng* **39**, 49–58.

Received 20 November 1996; accepted 20 March 1997

PHILOSOPHICAL TRANSACTIONS OF THE ROYAL SOCIETY B BIOLOGICAL SCIENCES